Multipotent Peripheral Glial Cells Generate Neuroendocrine Cells of the Adrenal Medulla

A. Furlan[&,1], **V. Dyachuk**[&,2,3,4], **M. E. Kastriti**[&,5], **L. Calvo-Enrique**[1], **H. Abdo**[1], **S. Hadjab**[2], **T. Chontorotzea**[5], **N. Akkuratova**[6,7], **D. Usoskin**[1], **D. Kamenev**[2], **J. Petersen**[5,8], **K. Sunadome**[5], **F. Memic**[1], **U. Marklund**[1], **K. Fried**[2], **P. Topilko**[9], **F. Lallemend**[2], **P. V. Kharchenko**[10], **P. Ernfors**[#,1], and **I. Adameyko**[#,5,8]

[1]Unit of Molecular Neurobiology, Department of Medical Biochemistry and Biophysics, Karolinska Institutet, 17177 Stockholm, Sweden

[2]Department of Neuroscience, Karolinska Institutet, 17177 Stockholm, Sweden

[3]National Scientific Center of Marine Biology, Far Eastern Branch, Russian Academy of Sciences, 690041, Vladivostok, Russia

[4]Department of Nanophotonics and Metamaterials, ITMO University, St Petersburg 197101, Russia

[5]Department of Physiology and Pharmacology, Karolinska Institutet, 17177 Stockholm, Sweden

[6]Skolkovo Institute of Science and Technology, 143005 Moscow, Russia

[7]Institute of Translational Biomedicine, St. Petersburg State University, 199034 St. Petersburg, Russia

[8]Center for Brain Research, Medical University Vienna, 1090 Vienna, Austria

[9]Institut de Biologie de l'Ecole Normale Supérieure (IBENS), Ecole Normale Supérieure, INSERM U 1024, CNRS UMR 8197, 46 rue d'Ulm, 75005, Paris, France

[10]Department of Biomedical Informatics, Harvard Medical School, MA 02115 Boston, USA

Abstract

Adrenalin is a fundamental circulating hormone for bodily responses to internal and external stressors. Chromaffin cells of the adrenal medulla (AM) represent the main neuroendocrine adrenergic component and are believed to differentiate from neural crest cells. Here, we demonstrate that large numbers of chromaffin cells arise from peripheral glial stem cells, termed Schwann cell precursors (SCPs). SCPs migrate along the visceral motor nerve to the vicinity of the forming adrenal gland where they detach from the nerve and form post-synaptic neuroendocrine chromaffin cells. An intricate molecular logic drives two sequential phases of gene expression, one unique for a distinct transient cellular state and another for cell-type specification. Subsequently, these programs downregulate SCP- and upregulate chromaffin-cell-gene networks. The adrenal

---

[*]Correspondence to: patrik.ernfors@ki.se; igor.adameyko@ki.se.
[&]equal contribution
[#]corresponding co-senior authors

medulla forms through limited cell expansion and requires the recruitment of numerous SCPs. Thus, peripheral nerves serve as a stem cell niche for neuroendocrine system development.

Chromaffin cells are neuroendocrine cells that produce catecholamines, which once released into the blood stream mediate a stress response in health and disease by regulating bodily organs and tissues, including effects on metabolism. Furthermore, neuroblastoma, the most common extracranial tumor in children, originates from the sympatho-adrenal compartment during development. Despite the functional importance of chromaffin cells, their origin and development is not well understood. Here, we revisited the embryonic origin of chromaffin cells and discovered a new chromaffin progenitor type i.e. the nerve-associated Schwann cell precursor (SCP).

Current opinion holds that the adrenergic chromaffin cells in the adrenal medulla (AM) originate from a migratory stream of neural crest cells that commit to a common sympatho-adrenal lineage located close to the dorsal aorta. Upon their arrival at the dorsal aorta region, the committed sympatho-adrenal cells proliferate and produce a spatial split in a dorso-ventral direction. The more ventral group of cells forms the AM, while the dorsal portion coalesces into a sympathetic ganglion (SG) (1, 2). However, this view is challenged by the discovery of early differential expression of markers in the sympatho-adrenal lineage (3, 4) and the presence of SOX10$^+$ satellite glial cells in the early sympathetic system at the time of adrenal anlagen formation (5, 6). Direct evidence on how the AM is formed is missing, and furthermore, the current idea does not explain the cellular origin of the suprarenal sympathetic ganglion (SRG), in direct association with the adrenal gland. Thus, it has not been clear whether progenitors committed to the sympatho-adrenal fate produce both sympathetic and chromaffin cells, or if SCPs and satellite glial cells also participate in the generation of chromaffin cells.

SCPs serve as multipotent stem cells which can differentiate into numerous cell types, and most or all of the parasympathetic nervous system arise from these cells (7–10). It appeared possible that chromaffin cells also could arise from SCPs since, like parasympathetic neurons, they are located inside of the organ where they function, and appear later in embryonic development in relation to neural crest stem cell migration.

SCPs build the adrenal medullae

To examine if SOX10$^+$ nerve-associated SCPs contribute to the generation of the main adrenergic sympathetic system we fate traced nerve-associated SCPs using neural crest and glia-specific inducible Cre lines *Sox10^{CreERT2}* and *Plp1^{CreERT2}* coupled to the *R26R^{YFP}* reporter. Genetic cell-fate tracing was initiated in SCPs by tamoxifen-induced recombination at E11.5 when neural crest cell migration is complete in the trunk (Fig. S1) and multiple derivatives have been produced. The analysis of medullas at E17.5 revealed big amounts of traced TH$^+$ chromaffin cells (Fig. 1A-C). Although initiating recombination at E12.5 demonstrated lower amounts of traced chromaffin cells, activation of recombination at E15.5 resulted in almost no contribution in E17.5 AM (Fig. 1B-C). At the same time, the contribution of traced cells to sympathetic neurons of the SRG, ganglia of the sympathetic chain as well as mesenteric or para-aortic ganglia was negligible (Fig. 1A-C; Fig. S2),

showing that the SCP compartment is restricted in terms of generating chromaffin cells versus sympathoblasts. Any neural crest recombination would be expected to result in fate-traced cells in the sympathetic system, thus, this finding also confirms the specificity of recombination in SCPs and not neural crest, consistent with the absence of freely migrating neural crest cells at these stages.

Given the recombination efficiency (Fig. 1B-C), we conclude from these experiments that at least half of all chromaffin cells are generated from nerve-associated SCPs between E11.5 and E15.5. In line with this, DTA (Diphtheria Toxin subunit A)-based ablation of SCPs performed in $Sox10^{CreERT2};R26R^{DTA}$ embryos injected twice with tamoxifen at E11.5 and E12.5 and analyzed at E13.5 or E17.5 revealed a reduction of Sox10$^+$ cells in both the SRG and the AM and TH$^+$ chromaffin cell depletion in the AM in contrast to the unaffected sympathoblast numbers (Fig. 1D-E; Fig. S3).

SCPs migrate along nerves, in contrast to the free migration of neural crest cells and common sympatho-adrenal progenitors. Thus, if chromaffin cells arise from SCPs, then formation of the AM should depend on the nerves innervating the gland. We therefore investigated the dependence of AM development on the presence of pre-ganglionic motor nerve fibers. Pre-ganglionic sympathetic motor neurons are located in the interomediolateral (IML) portion of the spinal cord. Fast blue retrograde tracing experiments previously identified NOS$^+$/CHAT$^+$ neurons as the source of AM innervation (11, 12). In order to achieve ablation of pre-ganglionic nerves, intersectional genetics were employed by breeding $HB9^{Cre}$ mice to the $Isl2^{DTA}$ mice. In these mice, DTA expression is driven by the $Isl2$ promoter. $Isl2$ and $Hb9$ expression is initiated in both somatic and visceral preganglionic neurons at E11.5 (13). $HB9^{Cre}$ mice were first bred to $R26R^{Tomato}$ reporter mice to generate $HB9^{Cre};R26R^{Tomato}$ embryos. Analysis of $HB9^{Cre};R26R^{Tomato}$ embryos at E15.5 revealed that $Hb9$ is expressed by NOS$^+$/ISL1$^+$ pre-ganglionic neurons and by their fibers in the adrenal gland (Fig. S4A,B) but expressed by 5% of all developing chromaffin cells (Fig. S4C,D). Furthermore, we did not detect the expression of $Isl2$ and $Hb9$ in developing AM using single cell transcriptomics. Thus, this approach allows for specific ablation of preganglionic motor neurons. At E14.5 only a few motor neurons were left in the spinal cord of $Hb9^{Cre};Isl2^{DTA}$ embryos (Fig. 2A,B and S4E). Analysis showed a reduction by 78% in the total number of AM cells in $Hb9^{Cre};Isl2^{DTA}$ mice (Fig. 2C-F), when compared to control mice, but the number of sympathetic neurons in the SRG was unaffected (Fig. 2E). The remaining chromaffin cells in $Hb9^{Cre};Isl2^{DTA}$ mice might be derived from the early neural crest streams or few remaining traversing visceral sensory afferent fibers, since both visceral and somatic motor nerves are eliminated in $Hb9^{Cre};Isl2^{DTA}$ model.

SCPs actively migrate along the nerves, as DiI tracing from the ventral root exit points in E11.5 embryos led to later emergence of DiI$^+$ cells within the AM region (Fig. S5A). Migration of SCP along nerves was also analyzed using genetic tracing. $Krox20$ ($Egr2$) is expressed exclusively in boundary cap cells located at the PNS/CNS border (14, 15) and these cells loose $Krox20$ expression when detaching from the cap and migrating towards various locations in the embryos. We used $Krox20^{Cre};R26^{RFP}$ mice to evidence that a few of these cells arrive to dorsal aorta and AM regions (Fig. S5B). Combined, these findings suggest that in contrast to sympathetic neurons origin directly from the migratory neural

crest, 77.8% of the AM chromaffin cells are generated by recruitment of SCPs, schematically illustrated in Fig. 2G.

If chromaffin cells are formed by the initiation of a chromaffin gene expression program in nerve-associated SCPs, then abolishing this transcriptional differentiation program would be expected to result in the accumulation of SCPs that fail to differentiate. To test this hypothesis, we examined mice deficient in $Ascl1$ - a critical factor driving chromaffin differentiation (16). Specifically, we generated $Ascl1^{CreERT2/CreERT2};R26R^{Tomato}$ mice, in which the insertion of two $CreERT2$ alleles generates a knock-out of $Ascl1$, allowing for genetic cell lineage tracing of $Ascl1^{-/-}$ cells. In control $Ascl1$ heterozygous mice ($Ascl1^{CreERT2/+};R26R^{Tomato}$), fate-traced $Ascl1^{TOM+}$ cells generated low numbers of S100β $^+$/SOX10$^+$/$Ascl1^{TOM+}$ Schwann cells and numerous S100β^-/SOX10$^-$/TH$^+$/PHOXB2$^+$/ $Ascl1^{TOM+}$ chromaffin cells, whereas in mice lacking $Ascl1$ ($Ascl1^{CreERT2/CreERT2};R26R^{Tomato}$ mice), $Ascl1^{TOM+}$ cells failed to down-regulate glial markers S100β and SOX10 (Fig. 3A-H). At the same time, numerous traced cells were found to initiate expression of the transcription factor PHOX2B that is part of the chromaffin differentiation program but failed to become catecholaminergic (i.e. SOX10$^-$/PHOX2B$^+$/TH $^-$) (Fig. 3H-J). Using serial sections, we quantified the frequency with which AM $Ascl1^{TOM+}$ traced cells remained as glial-like cells (SOX10$^+$), differentiated into chromaffin cells (TH$^+$/PHOX2B$^+$), or displayed the truncated chromaffin differentiation program with initiation of PHOX2B that, nevertheless, failed to become catecholaminergic (SOX10$^-$/ PHOX2B$^+$/TH$^-$). $Ascl1^{CreERT2/CreERT2};R26R^{Tomato}$ mice displayed a 5-fold increase in proportion and 6-fold increase in numbers of traced SOX10$^+$ cells, the appearance of SOX10$^-$/PHOX2B$^+$/TH$^-$ cells with simultaneous 55% reduction of TH$^+$ cell numbers (Fig. 3I-K). The accumulation of glial cells in the absence of a neurogenic program is consistent with a SCP origin of chromaffin cells.

Thus, our experiments using SCP fate tracing, SCP ablation, nerve ablation and interference of chromaffin differentiation are all consistent with an SCP origin of large numbers of chromaffin cells in the AM.

Lineage segregation of sympathoblasts and chromaffin cells

Sympathetic neurons and chromaffin cells have been considered to originate from a common sympatho-adrenal progenitor lineage located as a cluster of cells in the vicinity of the dorsal aorta. Our results indicate that large numbers of chromaffin cells are of a different cellular origin as compared to sympathetic neurons. This implies that the two lineages split at an earlier stage in development than previously thought. The primordium of AM forms around E12.5 and the earliest observations identifying the primary adrenal anlage is at E11.5 (1), and hence, the lineage split is expected at some time prior to this. To examine this, we performed a number of genetic cell-lineage tracing experiments. $Ascl1$ is expressed by both sympathetic and chromaffin cells, and the differential timing of its activation of expression can help to observe the lineage separation event. $Ascl1^{CreERT2/+};R26R^{Tomato}$ mice were injected with tamoxifen at E11.5 to fate trace $Ascl1$-expressing cells from this stage in development. Analysis of E17.5 embryos revealed that at E11.5, the lineages of sympathetic neurons and chromaffin cells were largely separated because most of AM cells were traced,

whereas only few paravertebral or SRG sympathetic neurons were TOM[+] (Fig. S6A). This indicated that at E11.5 sympathoblasts downregulated active transcription of *Ascl1* as compared to chromaffin progenitors and consequently, the lineages are separated at this time.

The tyrosine kinase RET is important for proper migration, proliferation and survival of sympathetic cells (17) and is expressed by neural crest, sympathoblasts as well as chromaffin cells at different developmental time points (18, 19). Whole mount (Fig. S6C) and cryosection-based immunohistochemical analysis (Fig. S6D-E) revealed RET expression in sympathetic progenitors and an absence of *Ret* expression in the vast majority of SCPs along the nerves of E11.5 embryos. *Ret*^{CreERT2} mice were bred to *R26R*^{Tomato} mice for cell fate tracing cells expressing *Ret* at E11.5 in *Ret*^{CreERT2};*R26R*^{Tomato} mice with analysis at E15.5. Both para-vertebral and SRG sympathetic neurons were traced, in contrast to minor tracing of AM cells (Fig. S6B). The same result was obtained with tamoxifen injections at E10.5 (Fig.4A,B), suggesting an early lineage split in progenitors generating sympathetic neurons and chromaffin cells.

Progenitors of sympathetic neurons express *Sox10* and *Plp1*, however the genes are downregulated during differentiation which starts at around E10.5 (20). Thus, tracing from the *Plp1* locus at this stage should help to further corroborate the lineage split at this early stage. Even though tracing in *Plp1*$^{CreERT2/+}$;*R26R*$^{YFP/+}$embryos injected with tamoxifen at E10.5 revealed more than 50% contribution to AM by E17.5, contribution to sympathetic ganglia (SG) and suprarenal ganglia (SRG) was no more than 10% (Fig. 4C,D).

Since many of early differentiating sympathoblasts are transiently exhibiting cholinergic phenotype (19), we analyzed *Chat*$^{Cre/+}$;*R26R*$^{YFP/+}$ embryos to rule out possible transition from sympathoblasts towards chromaffin cells of AM. We found no signs of conversion of maturing CHAT[+] sympathoblasts into chromaffin cells (Fig. 4E).

Taken together, all these data support an early lineage split between the sympathetic and the adrenal medulla chromaffin cells, following the completion of neural crest migration (Fig. 4F).

Gene-programs driving SCP specification into adrenergic cells

To obtain molecular insights into gene expression programs governing SCP-to-chromaffin cell transition, we performed single cell RNA sequencing of the developing adrenomedullary cells at E12.5 and E13.5, stages when chromaffin cells are first appearing. We labelled the entire neural crest-derived compartment using *Wnt1-Cre;R26R*^{Tomato} mice and sorted fluorescent single cells from dissected medullae with associated SRGs into 384-well plates for individual sequencing using Smart-seq2 protocol (21). The SRG was included to allow comparison of AM cells to sympathetic neurons. Analysis using pathway and gene set overdispersion analysis (PAGODA) (22) identified coordinated expression variability signatures separating distinct subpopulations of cells in both E12.5 and E13.5 samples in a statistically significant way (Fig. 5A,F and S7A-C). The two time points also showed a common subpopulation structure (Fig. 5B,G), with a prominent cluster of sympathoblasts

(purple), chromaffin cells (green) and a cluster of SCPs (blue). The SCPs were marked by high levels of *Foxd3, Sox10, Plp1* and *Erbb3*. ERBB3 is a part of heteromeric receptor complex in glial cells that is necessary for survival and proliferation of SOX10^{+}/PLP1^{+} SCPs receiving ligand interaction from membrane-anchored neuregulin-1 (NRG1) that is presented by the nerves (23). In the areas poor in NRG1, or after soluble NRG1 is not produced any longer (2), SOX10^{+} SCPs can maintain their survival and multiply only following the nerve branches that supply them with anchored NRG1. Reiprich and colleagues showed the presence of the SOX10^{+} cells in locations where the nerves normally descend to the AM, but the role of the nerve has not been explored (6). Consistently, nerves in the sympatho-adrenal area were confirmed to be NRG1^{+} (Fig. S8A). SOX10^{+} SCPs displayed expression of multiple genes participating in myelination (*Pou3f1/Oct6, Sh3tc2, Lgi4, Dhh, Mal, etc.*) and other glial cell markers (*Fabp7, Mpz* – coding for P0, *S100β, laminins, Mag*) (Fig. S8B-E).

The sympathoblasts were distinguished by the presence of *Slc18a3* (19) and *Cartpt* (coding for CART) (4) as well as by broader markers of sympatho-adrenal differentiation such as *Th* and chromaffin cells were identified by a *Th[+]/Phox2b^{+}/Chgb[+]/Slc18a3[−]/Cartpt[−]* signature (Fig. 5C,H and Fig. S7B-D) (4).

The remaining subpopulations (red and yellow in Fig. 5B, G) were intermediate types of cells spanning the expression state space between SCP-like to more chromaffin-like cells. The greatest observed overt difference between red and yellow subpopulations was the cell cycle signature present in the yellow cluster, but absent from the red cluster (Fig. 5C,H). To validate if expression of cell cycle genes causes the separation of these apparently two different cell types we normalized for cell cycle-associated genes and reanalyzed the dataset. With an omission of the cell cycle-related genes, the two identified populations (red and yellow, Fig 5B,G) closely aligned with each other (Fig. 5K,L). These intermediate cells form a continuous "bridge" between the chromaffin and SCP clusters, suggesting that they capture the transcriptional transition between SCP and chromaffin fates. In contrast, no such continuous "bridge" was observed between SCPs and sympathoblast clusters neither between chromaffin cells and sympathoblasts (Fig. 5B,G,K,L).

To examine the transcriptional transition from SCP to chromaffin cells, we carried out a pseudotime analysis (see Methods), positioning cells along a differentiation trajectory, and identifying genes that show statistically significant expression variation along this reconstructed differentiation time course (Fig. 5D,I). In addition to genes that are up- or down-regulated at the beginning or the end of the SCP-chromaffin path, we found a set of genes that were transiently increased specifically in differentiating cells, upregulated at different intermediate time points along this differentiation trajectory (Fig. 5D-J, 6A, S7B-C and supplementary Tables S1 and S2), but were not expressed in SCPs or chromaffin cells (Fig. 5D-J, S7B-C and supplementary Tables S1 and S2). This indicates the existence of an intermediate transient cellular state and that a complex regulatory cascade takes place within the "bridge" structure connecting SCPs and chromaffin cells. In the beginning of the pseudotime axis, SCP-specific genes *FoxD3*, *Sox10*, *Erbb3* and others were downregulated as cells moved into the *Ascl1^{+}/Htr3a^{+}* intermediate "bridge" state, towards chromaffin differentiation (*Th[+]/Chga[+]*) (Fig. 5D,E,I,J). Analysis of mitotic signatures showed

prevalence of cell divisions only in the first half of the SCP-chromaffin trajectory (Fig. 5C,H,K,L). In addition, ~300 of "bridge"-characterizing, transiently-expressed, genes defined the transition state including transcription factor (TF) signature (*Sox11, Hes6, Hipk2, Ascl1, Btg2, Aes* etc.) and signaling-related modules (*Dll, PlxnA2, Htr3a, Htr3b, Cdkn1c, Kcnj12* etc.) (Fig. 6A, S7B). Numerous TFs and signaling genes (SiGs) demonstrated affinity to the first (TFs: *Tcf3, Smo, Id3, Ybx1, Sox4* etc. SiGs: *Notch1, Fzd2, Ptk7* etc.) or the second half (TFs: *Hand1, Hand2, Phox2a, Eya1, Thra, Gata3, Insm1, Tbx20, Tlx2* etc. SiGs: *PlxnA3, Dll4, Amer2, Cxxc4* etc.) of the SCP-to-chromaffin trajectory. Towards the end of the pseudotime trajectory, we observed a group of specific genes indicative of the final steps of chromaffin differentiation beyond *Th* and *Chga* (TFs: *FoxQ1, Egr1, Elf4* etc. SiGs: *Nrp2* etc.) (Fig. S7B,D). Furthermore, numerous genes showed expression specific to the chromaffin subpopulation and clearly differentiated chromaffin cells from sympathoblasts (*Bhlhe40, Sox1, Adora2*) (Fig. S7D and Table S3).

Overall, among the genes showing statistically significant association with the SCP-chromaffin differentiation trajectory, we found 139 transcription factors and 60 molecules from well-understood signaling pathways (Fig. S7B).

These results show a mechanism involving a progressive down-regulation of SCP genes and upregulation of chromaffin genes, starting with *Phox2b, Ascl1*, passing through transient stages and culminating with the induction of effector genes such as *Th* and *Chga*. Studies have demonstrated that ASCL1 and PHOX2B are critical transcription factors during formation of sympathetic (24), parasympathetic (9) nervous systems, and adrenal gland development (16). The Gene Ontology annotations showed statistically significant over-representation of differentially-expressed genes from NOTCH, TGFβ, canonical WNT and Sonic signaling pathways at various steps of SCPs-to-chromaffin transition (Fig. S9).

In situ existence of SCP cells in transit to generate adrenergic AM cells

Equipped with new and old markers for SCPs, "bridge" cells and adrenergic chromaffin cells we next examined the dynamics resulting in the formation of the AM cells within the tissue. The steroidogenic precursors that form the adrenal cortex are present at E11.5 and are revealed by steroidogenic factor-1 (*Sf1*) expression. SF1$^+$ cells started at this stage to coalesce to form the adrenal cortex (Fig. 6B-C, S6D). At this time, *Ascl1*$^{TOM+}$, PHOX2B$^+$ and TH$^+$ cells, e.g. chromaffin cell progenitors, first appear in association with preganglionic sympathetic CHAT$^+$ nerves in the prospective location of AM (Fig. 6B). Injection of TAM in E10.5 *Ascl1*$^{CreERT2/+}$;*R26R*^{Tomato} embryos and analysis at E11.5 showed that some *Ascl1*$^{TOM+}$ cells were expressing *Th* whereas others *Ascl1*$^{TOM+}$ cells expressed the SCP markers *Sox10* and *Erbb3*. Interestingly, *Ascl1*$^{TOM+}$/TH$^+$ cells were retaining some levels of *Sox10* expression (Fig. 6B) suggesting that glial program (i.e. SOX10) downregulation precedes the commitment to the chromaffin cell fate, consistently with single cell transcriptomics data. In line with this, nerve-associated TH$^+$ cells were not ERBB3$^+$ at E11.5 or E12.5 (Fig. 6B,D), consistent with the single cell transcriptomics analysis (Fig. 5E,J) and confirming that *Erbb3* expression is extinguished prior to a putative SCP-to-chromaffin fate switch.

We next identified cells in the SCP-to-chromaffin intermediate "bridge" stage (red and yellow clusters on t-SNE plots in Fig. 5B,G) using the marker *Htr3a*. In order to detect *Htr3a*-expressing cells, we took advantage of the *Htr3a*^{EGFP} reporter mouse line. Analysis of E11.5 embryos confirmed the existence of *Htr3a* expressing (EGFP$^+$) cells, most of which appeared to be nerve-associated and negative for TH as early as E11.5 in the AM region (Fig. 6C). The small number of weakly EGFP$^+$ cells also stained for TH is likely caused by the slow degradation of EGFP molecules. The EGFP$^+$ cells displayed variable levels of *Sox10* expression at all analyzed stages (Fig. 6C-D, S7E). In order to visualize cells in transition from SCPs to chromaffin cells between E12.5 and E13.5 we performed lineage tracing using *Sox10*^{CreERT2};*R26R*^{YFP} mice. Numerous traced SOX10$^+$ cells of AM were PHOX2B$^+$, which is a key transcription factor driving the adrenergic fate. By contrast, in sympathetic ganglia, traced SOX10$^+$ cells were negative for PHOX2B$^+$ (Fig. S7F-G). This agrees with the single cell transcriptomics data where *Phox2b* expression is predicted early among SOX10$^+$ cells entering the "bridge" stage (Fig. S7B). Quantification of cells in transit to adopt a chromaffin cell fate by measuring the number of *Htr3a*$^{EGFP+}$/TH$^-$ cells revealed chromaffin cell differentiation of SCPs to occur at E11.5, with a peak at E12.5 and decline at E13.5 (Fig. 6D-E, Fig. S7H), consistent with our cell fate tracing of SCPs. Taking advantage of this, we conducted whole embryo 3D rendering at E12.5 to identify the intermediate "bridge" cells in the intact tissue. For this purpose we used a combination of various markers such as PHOX2B$^+$ to detect sympathetic and chromaffin progenitors, TH for differentiated sympathetic and chromaffin cells, Neurofilament (NF) to detect sensory nerves of dorsal root ganglia (DRG), RET to detect early sympathetic progenitors and CART (coded by *Cartpt*) was used to detect the sympathetic component (chromaffin progenitors are CART$^-$). Finally, *Htr3a*$^{EGFP+}$ was used to identify intermediate "bridge" cells.

Two separate rostro-caudal extensions of PHOX2B$^+$/*Ret*$^{CFP+}$ sympathetic progenitor cells above and below dorsal aorta were identified at E11.5. The dorsal extension of cells represents the paravertebral sympathetic chain whereas the ventral population largely reflects para-aortic and suprarenal ganglia, coalescing as early as E11.5 based on the *Ret*$^{CFP+}$ profile (Fig. S6C). The identification of a parallel ventral sympathetic chain-like structure challenges the current idea that the ventral portion represents only chromaffin progenitors. Based on the mutually exclusive expression of *Cartpt* in sympathetic cells but not in the AM, and also having *Htr3a*^{GFP} expressed by intermediate "bridge" cells, we used 3D reconstructions to identify the "bridge" intermediate cells within the ventral PHOX2B$^+$/TH$^+$/CART$^-$ population at E12.5 (Fig. 6F-I).

"Bridge" and differentiating chromaffin cells showed an increasing expression of nicotinic cholinergic receptors based on single cell RNA sequencing. This could suggest the role of the cholinergic signaling (25) in AM development (Fig. S10A,B). To evidence a putative role of the cholinergic signaling for adrenergic differentiation, we isolated the AM from the embryos at E12.5 and E13.5 and cultivated them separately for 24-48 hours in the presence of activators or inhibitors of nicotinic receptors. The analysis (including 3D measurements) showed that SOX10$^+$ and TH$^+$ cells appear in denervated and isolated medullae equally well in all conditions, suggesting that cholinergic signaling is not a key for the early steps of medulla formation. However, the levels of *Th* expression were found higher in conditions with inhibitors (by 45% in the free-floating and 30% in the membrane-cultured AM

explants, Fig. S10C-H), suggesting that the nerve activity may play a role in scaling the production of catecholamines by chromaffin cells by regulating the related enzymatic pathways.

Cell dynamics during adrenal medulla organogenesis

The different cellular origin and molecular process of sympathetic neurons and chromaffin cells opens for possible differences in mechanisms of tissue expansion during organogenesis. Organs can be built by few cells expanding massively or many cells expanding modestly.

We made use of the *pTRE-H2BGFP;rtTA* transgenic mouse line to examine proliferation of cells during the formation of the AM. In this mouse strain, histone H2B is fused to GFP. Because the number of histones is doubled at every cell division, a transient expression of *H2BGFP* is rapidly diluted if cells expand robustly, and hence the intensity of GFP correlates with the number of cell divisions after a doxycycline pulse (Fig. S11A). In embryos injected at E11.5 and analyzed at E12.5, *H2BGFP* retention was high in already fated TH^{+} chromaffin cells and low in ERBB3^{+} SCPs and the reverse was observed when embryos were injected at E13.5 and analyzed at E14.5 (Fig. S11A). This finding was substantiated by immunofluorescent analysis of KI67 (*Mki67*) expression, a marker for dividing cells. At E12.5 most SOX10^{+} cells were largely KI67^{+} whereas TH^{+} cells were KI67^{−}, consistent with our analysis of single cell RNA sequencing data (Fig. 5C,H,K,L). Conversely, at E14.5 and E17.5 the reverse was observed (Fig. S11B). The transient arrest in the proliferation of early differentiated TH^{+} chromaffin cells is similar to that previously reported in developing sympathetic ganglia (4, 20).

Thus, the AM is formed in two consecutive steps. The first phase of organogenesis involves an expansion of SCPs which deposits through differentiation a number of quiescent chromaffin cells in the AM. In the second phase, chromaffin cells expand in numbers by proliferation.

This finding prompted us to establish the number of chromaffin cells deposited from individual progenitors into the AM by each progenitor cell, revealing how many cell divisions take place to generate the AM. To achieve this, we took advantage of clonal genetic tracing with color-coding of neural crest clones using the *R26R^Confetti* reporter (26) coupled to *Sox10^CreERT2* injected with tamoxifen at E8.5. To achieve our objective, we used an experimental paradigm, which results in rare recombination events that when combined with the stochastic generation of different traceable color-codes following recombination in the Confetti mice, allows for clonal analysis. The analysis of AM and adjacent SRG from clonal density-traced embryos at E17.5 revealed the presence of color-coded clones (Fig. S11C and S12) that were comprised by less than 32 cells per medulla (with mean at 14 cells ± 1.8 shown in Fig. S11E). Spatial structure of the average clone demonstrated the presence of few cellular clusters often separated from each other by some distance. Numerous clones were unique for each system, even though some cells labelled by the same color-code were shared between AM and SRG (Fig. S12). This shows that chromaffin cells in medulla and sympathetic neurons in adjacent SRG might originate from different single neural crest cells

traced from E8.5 although the interpretation of these results requires caution since neural crest progeny can migrate up to six segments in rostrocaudal direction (27).

Next, we utilized *Sox10^CreERT2;R26R^Confetti* animals to trace SCPs in a low density-tracing mode starting from E11.5. Analysis at E17.5 showed that clones of chromaffin cells (originating from SCPs) were represented by less than 20 TH$^+$ cells (with mean number of cells per medulla = 10 ± 1.2, Fig. S11E). These cells often shared the clonal color-code with local SOX10$^+$ glial cells (Fig. S11D, arrows) and were organized into discrete spatial clusters comprised of 2-6 chromaffin and glial cells (Fig. S11F-H). Thus, the SCP-to-chromaffin cell conversion ratio is estimated to be one SCP cell labelled at E11.5 per approximately ten identified traced chromaffin cells at E17.5. These ratios are valid only until E17.5, since chromaffin cell proliferation continues into postnatal stages (28). Therefore, our results suggest that numerous SCPs are required to build the AM during embryogenesis.

Conclusions

Our findings represent the discovery of the SCP-dependent origin of chromaffin cells and explain the fate split between the sympathetic and adrenergic lineages, especially considering previously published data on clonal tracing of neural crest in sympatho-adrenal domain (29, 30). The difference in immediate origin and related timing of progenitor recruitment might define the split between sympathetic and chromaffin fates instead of a spatial heterogeneity of inductive signal.

Taken together, our results expand the diversity of SCP-derived cell types beyond previously known derivatives such as parasympathetic (9, 10) enteric neurons (31, 32), melanocytes (8), endoneural fibroblasts (33), mesenchymal stem cells (34, 35) and adult glial cells (36). Our findings show that the peripheral nerves are niches and transportation routes for progenitors essential also for neuroendocrine development. In fact, the nerve-ablation experiment demonstrates that high amounts of chromaffin cells are derived from the nerve, since the AM of nerve-ablated mice contained 78% less cells as compared to control. The knowledge gained in this study on cell types, their proliferative status, transcriptome and how they contribute to the generation of chromaffin cells in the AM helps not only to understand the origin of the adrenergic system, but could also be helpful in advancing our knowledge on neuroblastoma and pheochromatocytoma as these most often arise from the adrenal gland region (37). We have discovered that SCPs generate chromaffin cells via an intermediate progenitor cell type, a "bridge" cell, characterized by a specific transcriptional program. Thus, the identification of novel adrenal progenitors, SCPs and "bridge" cells, might help in understanding the origin of neuroblastoma and pheochromocytoma (for *MycN* expression in SCPs and "bridge" cells see Fig. S7C).

In an evolutionary context, a direct contribution from neural crest cells together with indirect contribution through SCPs may explain how the AM can be adaptively scaled in a species-specific manner. This idea agrees with results by Green et al, showing a marked change through evolution in the contribution of SCPs as progenitors during formation of the enteric

nervous system (38). Thus, it is possible that SCPs represent an evolutionary substrate cell type essential for the advancement of neuroendocrine system in the vertebrate lineage.

Supplementary Material

Refer to Web version on PubMed Central for supplementary material.

Acknowledgments

References

1. Huber K, Kalcheim C, Unsicker K. The development of the chromaffin cell lineage from the neural crest. Auton Neurosci. 2009; 151:10–16. [PubMed: 19683477]

2. Saito D, Takase Y, Murai H, Takahashi Y. The dorsal aorta initiates a molecular cascade that instructs sympatho-adrenal specification. Science. 2012; 336:1578–1581. [PubMed: 22723422]

3. Ernsberger U, et al. Expression of neuronal markers suggests heterogeneity of chick sympathoadrenal cells prior to invasion of the adrenal anlagen. Cell Tissue Res. 2005; 319:1–13. [PubMed: 15565470]

4. Chan WH, et al. Differences in CART expression and cell cycle behavior discriminate sympathetic neuroblast from chromaffin cell lineages in mouse sympathoadrenal cells. Dev Neurobiol. 2016; 76:137–149. [PubMed: 25989220]

5. Gut P, et al. Lack of an adrenal cortex in Sf1 mutant mice is compatible with the generation and differentiation of chromaffin cells. Development. 2005; 132:4611–4619. [PubMed: 16176945]

6. Reiprich S, Stolt CC, Schreiner S, Parlato R, Wegner M. SoxE proteins are differentially required in mouse adrenal gland development. Mol Biol Cell. 2008; 19:1575–1586. [PubMed: 18272785]

7. Adameyko I, Ernfors P. Nerves transport stem-like cells generating parasympathetic neurons. Cell Cycle. 2014; 13:2805–2806. [PubMed: 25486464]

8. Adameyko I, et al. Schwann cell precursors from nerve innervation are a cellular origin of melanocytes in skin. Cell. 2009; 139:366–379. [PubMed: 19837037]

9. Dyachuk V, et al. Neurodevelopment. Parasympathetic neurons originate from nerve-associated peripheral glial progenitors. Science. 2014; 345:82–87. [PubMed: 24925909]

10. Espinosa-Medina I, et al. Neurodevelopment. Parasympathetic ganglia derive from Schwann cell precursors. Science. 2014; 345:87–90. [PubMed: 24925912]

11. Appel NM, Elde RP. The intermediolateral cell column of the thoracic spinal cord is comprised of target-specific subnuclei: evidence from retrograde transport studies and immunohistochemistry. J Neurosci. 1988; 8:1767–1775. [PubMed: 2896766]

12. Dun NJ, Dun SL, Wu SY, Forstermann U. Nitric oxide synthase immunoreactivity in rat superior cervical ganglia and adrenal glands. Neurosci Lett. 1993; 158:51–54. [PubMed: 7694200]

13. Thaler JP, et al. A postmitotic role for Isl-class LIM homeodomain proteins in the assignment of visceral spinal motor neuron identity. Neuron. 2004; 41:337–350. [PubMed: 14766174]

14. Maro GS, et al. Neural crest boundary cap cells constitute a source of neuronal and glial cells of the PNS. Nat Neurosci. 2004; 7:930–938. [PubMed: 15322547]

15. Gresset A, et al. Boundary Caps Give Rise to Neurogenic Stem Cells and Terminal Glia in the Skin. Stem Cell Reports. 2015; 5:278–290. [PubMed: 26212662]

16. Huber K, et al. Development of chromaffin cells depends on MASH1 function. Development. 2002; 129:4729–4738. [PubMed: 12361965]

17. Enomoto H, et al. RET signaling is essential for migration, axonal growth and axon guidance of developing sympathetic neurons. Development. 2001; 128:3963–3974. [PubMed: 11641220]

18. Allmendinger A, Stoeckel E, Saarma M, Unsicker K, Huber K. Development of adrenal chromaffin cells is largely normal in mice lacking the receptor tyrosine kinase c-Ret. Mech Dev. 2003; 120:299–304. [PubMed: 12591599]

19. Furlan A, Lubke M, Adameyko I, Lallemend F, Ernfors P. The transcription factor Hmx1 and growth factor receptor activities control sympathetic neurons diversification. EMBO J. 2013; 32:1613–1625. [PubMed: 23591430]

20. Gonsalvez DG, et al. Proliferation and cell cycle dynamics in the developing stellate ganglion. J Neurosci. 2013; 33:5969–5979. [PubMed: 23554478]

21. Picelli S, et al. Full-length RNA-seq from single cells using Smart-seq2. Nat Protoc. 2014; 9:171–181. [PubMed: 24385147]

22. Fan J, et al. Characterizing transcriptional heterogeneity through pathway and gene set overdispersion analysis. Nat Methods. 2016; 13:241–244. [PubMed: 26780092]

23. Riethmacher D, et al. Severe neuropathies in mice with targeted mutations in the ErbB3 receptor. Nature. 1997; 389:725–730. [PubMed: 9338783]

24. Apostolova G, Dechant G. Development of neurotransmitter phenotypes in sympathetic neurons. Auton Neurosci. 2009; 151:30–38. [PubMed: 19734109]

25. Knox SM, et al. Parasympathetic innervation maintains epithelial progenitor cells during salivary organogenesis. Science. 2010; 329:1645–1647. [PubMed: 20929848]

26. Snippert HJ, et al. Intestinal crypt homeostasis results from neutral competition between symmetrically dividing Lgr5 stem cells. Cell. 2010; 143:134–144. [PubMed: 20887898]

27. Yip JW. Migratory patterns of sympathetic ganglioblasts and other neural crest derivatives in chick embryos. J Neurosci. 1986; 6:3465–3473. [PubMed: 3794784]

28. Jackson CM. The postnatal development of the suprarenal gland—and the effects of inanition upon its growth and structure in the albino rat. Amer J Anat. 1919; 25:220–289.

29. Krispin S, Nitzan E, Kassem Y, Kalcheim C. Evidence for a dynamic spatiotemporal fate map and early fate restrictions of premigratory avian neural crest. Development. 2010; 137:585–595. [PubMed: 20110324]

30. Shtukmaster S, et al. Sympathetic neurons and chromaffin cells share a common progenitor in the neural crest in vivo. Neural Dev. 2013; 8:12. [PubMed: 23777568]

31. Uesaka T, Nagashimada M, Enomoto H. Neuronal Differentiation in Schwann Cell Lineage Underlies Postnatal Neurogenesis in the Enteric Nervous System. J Neurosci. 2015; 35:9879–9888. [PubMed: 26156989]

32. Laranjeira C, et al. Glial cells in the mouse enteric nervous system can undergo neurogenesis in response to injury. J Clin Invest. 2011; 121:3412–3424. [PubMed: 21865647]

33. Im K, et al. Effects of the polyphenol content on the anti-diabetic activity of Cinnamomum zeylanicum extracts. Food Funct. 2014; 5:2208–2220. [PubMed: 25051315]

34. Kaukua N, et al. Glial origin of mesenchymal stem cells in a tooth model system. Nature. 2014; 513:551–554. [PubMed: 25079316]

35. Isern J, et al. The neural crest is a source of mesenchymal stem cells with specialized hematopoietic stem cell niche function. Elife. 2014; 3:e03696. [PubMed: 25255216]

36. Jessen KR, Mirsky R, Salzer J. Introduction. Schwann cell biology. Glia. 2008; 56:1479–1480. [PubMed: 18803316]

37. Szabo PM, et al. Integrative analysis of neuroblastoma and pheochromocytoma genomics data. BMC Med Genomics. 2012; 5:48. [PubMed: 23106811]

38. Green SA, Uy BR, Bronner ME. Ancient evolutionary origin of vertebrate enteric neurons from trunk-derived neural crest. Nature. 2017; 544:88–91. [PubMed: 28321127]

39. Golding JP, Cohen J. Border controls at the mammalian spinal cord: late-surviving neural crest boundary cap cells at dorsal root entry sites may regulate sensory afferent ingrowth and entry zone morphogenesis. Mol Cell Neurosci. 1997; 9(5-6):381–396. [PubMed: 9361276]

40. Trapnell C, Cacchiarelli D, Grimsby J, Pokharel P, Li S, Morse M, Lennon NJ, Livak KJ, Mikkelsen TS, Rinn JL. The dynamics and regulators of cell fate decisions are revealed by pseudotemporal ordering of single cells. Nat Biotechnol. 2014; 32:381–386. published online Epub Apr. DOI: 10.1038/nbt.2859 [PubMed: 24658644]

41. Bendall SC, Davis KL, el Amir AD, Tadmor MD, Simonds EF, Chen TJ, Shenfeld DK, Nolan GP, Pe'er D. Single-cell trajectory detection uncovers progression and regulatory coordination in human B cell development. Cell. 2014; 157:714–725. published online EpubApr 24. DOI: 10.1016/j.cell.2014.04.005 [PubMed: 24766814]

42. Buettner F, Natarajan KN, Casale FP, Proserpio V, Scialdone A, Theis FJ, Teichmann SA, Marioni JC, Stegle O. Computational analysis of cell-to-cell heterogeneity in single-cell RNA-sequencing data reveals hidden subpopulations of cells. Nat Biotechnol. 2015; 33:155–160. published online EpubFeb. DOI: 10.1038/nbt.3102 [PubMed: 25599176]

43. Adameyko I, Lallemend F, Furlan A, Zinin N, Aranda S, Kitambi SS, Blanchart A, Favaro R, Nicolis S, Lubke M, Muller T, Birchmeier C, Suter U, Zaitoun I, Takahashi Y, Ernfors P. Sox2 and Mitf cross-regulatory interactions consolidate progenitor and melanocyte lineages in the cranial neural crest. Development. 2012; 139:397–410. published online EpubJan. DOI: 10.1242/dev. 065581 [PubMed: 22186729]

One Sentence Summary

Cells producing adrenalin are largely derived from nerve-associated Schwann cell precursors via an intermediate progenitor "bridge" cell.
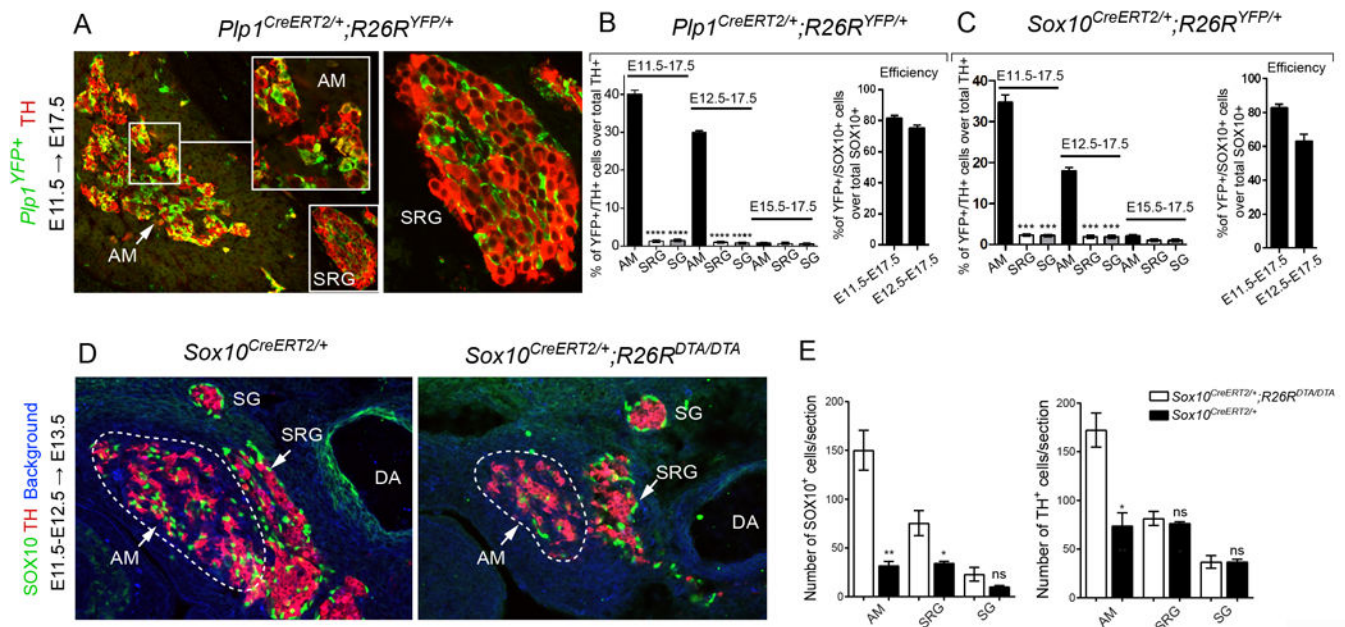
Fig. 1. Chromaffin cells of the adrenal gland originate from PLP1+ and SOX10+ Schwann cell precursors (SCPs) at E11.5 and E12.5

A. Immunohistochemistry for YFP (recapitulating *Plp1* expression) and TH on sections of the developing adrenal medulla (AM) and suprarenal ganglion (SRG) following genetic tracing in *Plp1^CreERT2/+;R26R^YFP/+* animals injected with TAM at E11.5 and analyzed at E17.5. The arrow points at the developing AM. **B-C.** Quantification of the proportion of TH^+/*Plp1^YFP+* cells traced in *Plp1^CreERT2/+;R26R^YFP/+* (**B**) and of TH^+/*Sox10^YFP+* cells in the AM, SRG and sympathetic ganglia (SG) of *Sox10^CreERT2/+;R26R^YFP/+* mice (**C**) injected at E11.5, E12.5 or E15.5 and analyzed at E17.5. Note that the recombination efficiency (percentage of SOX10^+/*Plp1^YFP+* cells out of all SOX10^+ cells in embryonic nerves) at E12.5 is lower than that at E11.5. **D.** Immunohistochemistry for SOX10 and TH on E13.5 sections of developing AM and SRG following tamoxifen (TAM)-induced cell ablation of SOX10^+ cells at both E11.5 and E12.5 in *Sox10^CreERT2/+;R26R^DTA/DTA* mice. Note the marked decrease in SOX10^+ and TH^+ cell numbers in *Sox10^CreERT2/+;R26R^DTA/DTA*embryos as compared to *Sox10^CreERT2/+;R26R^+/+*. **E.** Quantification of SOX10^+ and TH^+ cell numbers identified in the AM, SRG and SG of *Sox10^CreERT2/+;R26R^DTA/DTA* and *Sox10^CreERT2/+;R26R^+/+*embryos. Data are presented as mean ± s.e.m., two-tailed Student t-test. In **A-C**, for injection at E11.5: n=3, at E12.5: n=4 and at E15.5: n=3. In **D-E**, for *Sox10^CreERT2/+;R26R^+/+* and *Sox10^CreERT2/+;R26R^DTA/DTA* AM n=3, SRG n=4, SG n=3. AM: adrenal medulla; SRG: suprarenal ganglion; SG: sympathetic ganglion; ns: non-significant.

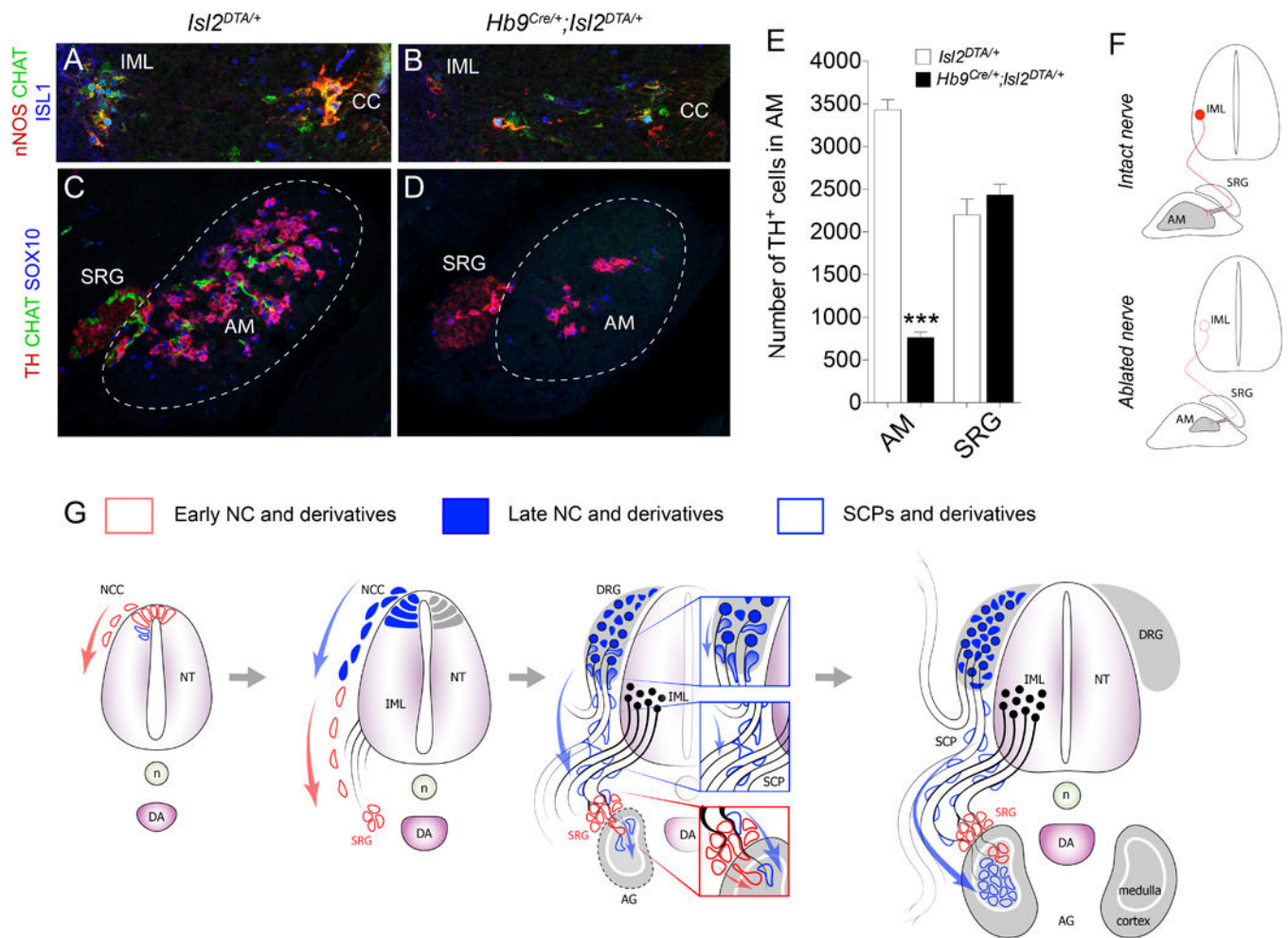**Fig. 2. Pre-ganglionic nerves are necessary for adrenal medulla assembly**

A,B Immunohistochemistry for nNOS, CHAT and ISL1 on E14.5 sections of spinal cords from control *Isl2^DTA/+* (**A**) and *Hb9^Cre/+;Isl2^DTA/+* embryos (**B**) show almost complete ablation of CHAT$^+$/nNOS$^+$/ISL1$^+$ pre-ganglionic neurons. **C, D.** Immunohistochemistry for TH, SOX10 and CHAT on E14.5 sections of adrenal medulla (AM) from control *Isl2^DTA/+* (**C**) and nerve-ablated *Hb9^Cre/+;Isl2^DTA/+* embryos (**D**). Note the significant reduction of chromaffin cells in the AM, but not of suprarenal ganglion (SRG) sympathetic neurons in nerve-ablated (**D**) compared to control (**C**) embryos. (**E**). Quantification of **C**, **D**. Data are presented as mean ± s.e.m., n=3 for *Isl2^DTA/+*, n=5 for *Hb9^Cre/+;Isl2^DTA/+*, two-tailed Student t-test. **F.** Graphical summary of the results. **G.** Schematic showing the origin of chromaffin cells from nerve-associated SCPs. IML: intermediolateral cell column; CC: central canal; AM: adrenal medulla; AG: adrenal gland; SRG: suprarenal ganglion; NCC: neural crest cells; NC: neural crest; NT: neural tube; n: notochord; DA: dorsal aorta; DRG: dorsal root ganglion; SCPs: Schwann cell precursors.
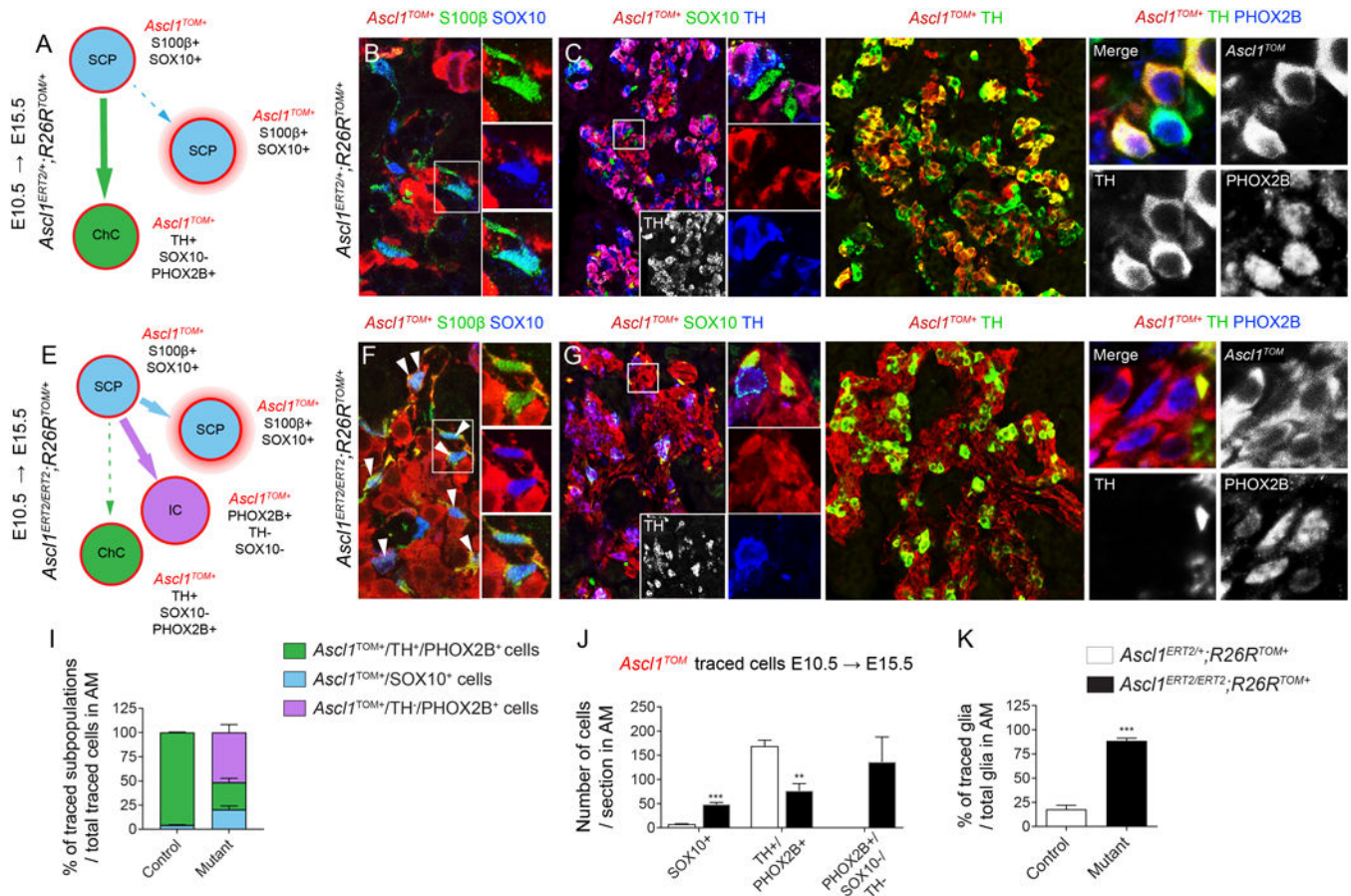
Figure 3. The role of *Ascl1* in the SCP-to-chromaffin transition
A-H Genetic ablation of *Ascl1* prevents the glia-to-chromaffin transition. The majority of nerve-associated SOX10$^+$/S100β$^+$ cells expressing *Ascl1* at E10.5 downregulated glial markers in *Ascl1$^{CreERT2/+}$;R26R$^{TOM/+}$* (control) embryos at E15.5 and have differentiated towards TH$^+$/PHOX2B$^+$ chromaffin cells (**A,B,C**) but failed to do so in *Ascl1*-deficient *Ascl1$^{CreERT2/CreERT2}$;R26R$^{TOM/+}$* (mutant) embryos (**E,F,G**), while a new, intermediate PHOX2B$^+$/TH$^-$/SOX10$^-$ population is observed (**D,H**). **I,J.** The majority of *Ascl1^{TOM+}* cells in *Ascl1$^{CreERT2/+}$;R26R$^{TOM/+}$* embryos are chromaffin cells with a minor contribution to SOX10$^+$ glia, while in the *Ascl1*-deficient *Ascl1$^{CreERT2/CreERT2}$;R26R$^{TOM/+}$* embryos the larger population is represented by PHOX2B$^+$/TH$^-$/SOX10$^-$ cells with simultaneous increase in SOX10$^+$ glia and reduction in TH$^+$/PHOX2B$^+$ chromaffin cells. **K.** The proportion of *Ascl1^{TOM+}*/SOX10$^+$ glia over the total glia population is significantly increased in the mutant. Note the complete absence of the *Ascl1^{TOM+}*-traced PHOX2B$^+$/TH$^-$/SOX10$^-$ population in the control, which is observed in the mutant. Data presented as mean ± s.e.m., n=3 for all cases, two-tailed Student t-test. In **A** and **E**, the main differentiation trajectories derived from Schwann cell precursors (SCPs – marked with a pink halo) are shown with big arrows, while trajectories producing a minor or reduced cell population are shown by dashed arrows. White arrowheads point to *Ascl1^{TOM+}* glial cells. SCP: Schwann cell precursor; ChC: chromaffin cell; IC: intermediate cell; AM: adrenal medulla.
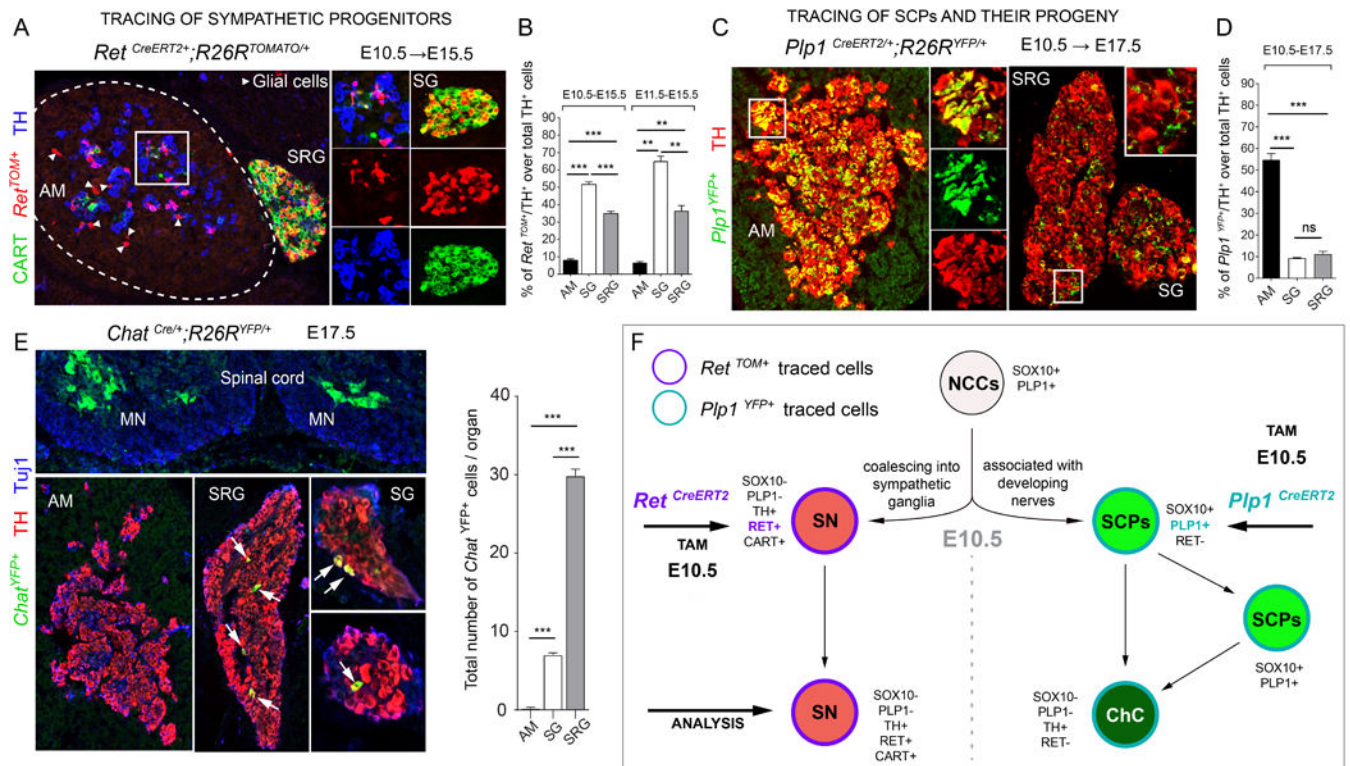
Figure 4. Early specification and separation of sympathoadrenal lineages during development
A. Immunohistochemistry for TOMATO (recapitulating *Ret* expression) on *Ret*^{CreERT2/+};*R26R*^{TOM/+}embryos injected with TAM at E10.5 and analysed at E15.5. Arrowheads point to traced glia. **B.** Analysis of *Ret* tracing in the adrenal medulla (AM), sympathetic ganglion (SG) and suprarenal ganglion (SRG) in *Ret*^{CreERT2/+};*R26R*^{TOM/+}embryos injected with TAM at E10.5 or E11.5 and analysed at E15.5. Note the high recombination in the SG and SRG (for E10.5 injection: 51.77±1.40% in the SG, 35.05±1.19% in the SRG; for E11.5 injection: 64.96±3.01% in the SG, 36.4±3.08% in the SRG) in contrast to the AM (for E10.5 injection: 8.09±0.71%; for E11.5 injection: 6.54±0.72%). **C.** Immunohistochemistry for YFP (recapitulating *Plp1* expression) and TH on *Plp1*^{CreERT2/+}/*R26R*^{YFP/+} embryos injected with TAM at E10.5 and analyzed at E17.5. Note high numbers of *Plp1*^{YFP+}/TH⁺ cells in the AM but only a few in the SG and SRG. **D.** Quantification of C. Note the high recombination in the AM (54.60±3.01%) in contrast to the SG and SRG (9.23±0.22% and 11.05±1.37% respectively). **E.** Immunohistochemistry for YFP (recapitulating *Chat* expression), TH and TuJ1 on *Chat*^{Cre/+};*R26R*^{YFP/+} embryos analyzed at E17.5. Arrows point to *Chat*^{YFP+} cells in the SRG and SG. **F.** Schematic showing the fate restriction of neural crest cells towards sympathetic neurons and Schwann cell precursors, finally differentiating into chromaffin cells. In **B,D,E** data are presented as mean ± s.e.m., n=3 for all cases, two-tailed Student t-test. SG: sympathetic ganglion; SRG: suprarenal ganglion; AM: adrenal medulla; DRG: dorsal root ganglion; MN: motoneurons; TAM: tamoxifen; NCCs: neural crest cells; SN: sympathetic neurons; SCPs: Schwann cell precursors; ChC: chromaffin cell.
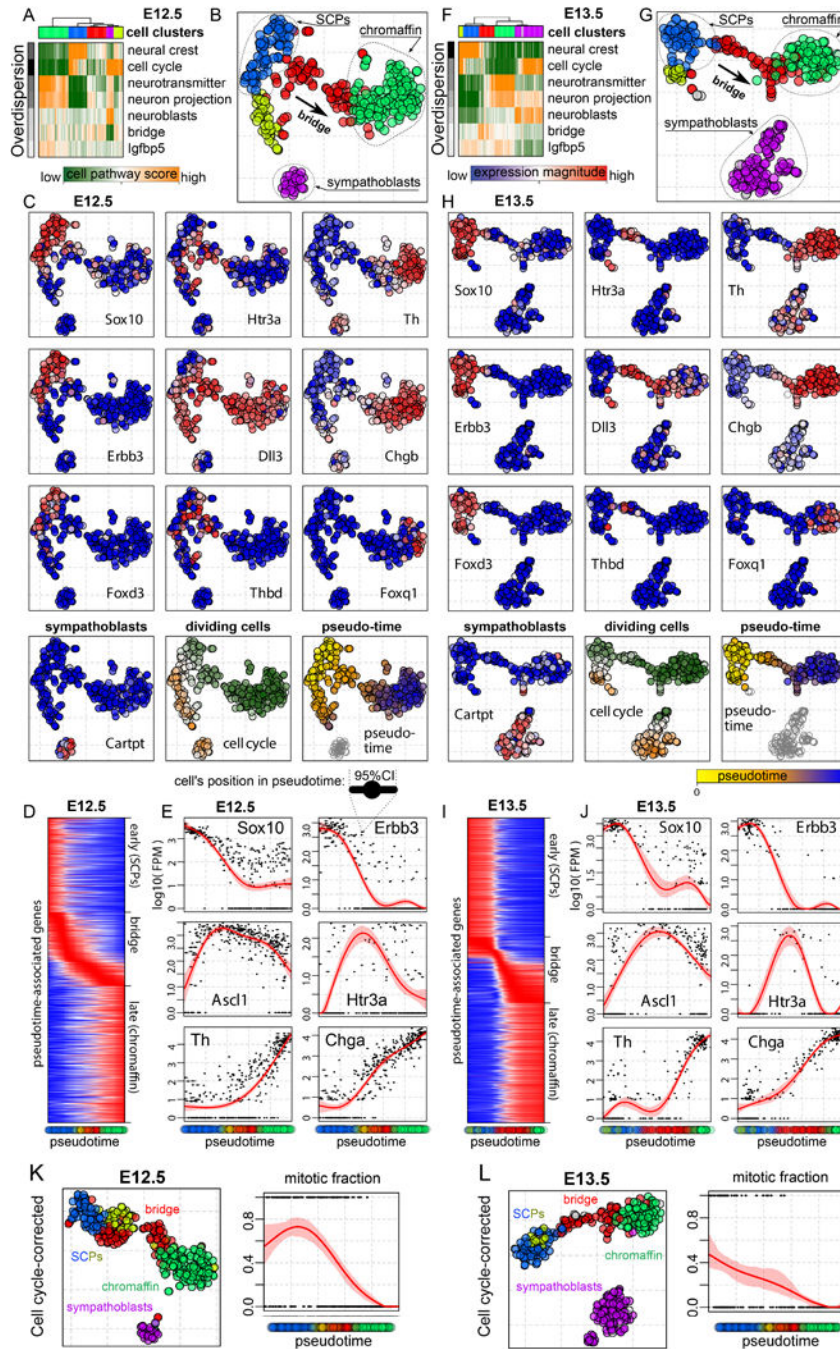
Fig. 5. Transcriptional heterogeneity of the developing adrenal medulla demonstrates SCP-to-chromaffin fate transition through a defined "bridge" state

A. Distinct subpopulations of neural crest-derived cells (columns) are seen within the E12.5 adrenal medulla (AM). Top 5 clusters of cells are given by the color bar below the dendrogram. Top 7 statistically significant aspects (rows) of transcriptional heterogeneity are shown, labelled according to the main GO category or a key gene driving each aspect. **B.** Transcriptional profile-based subpopulations in the E12.5 sample are visualized using t-SNE embedding. The labels show interpretation of the distinct subpopulations based on the key marker genes below, and a continuous "bridge" cell population (in red) connecting the SCPs

and the chromaffin clusters. **C**. Expression levels of representative marker genes within the E12.5 population (first 10 plots). Cell cycle dynamics ("dividing cells": yellow – mitotic, green – interphase) are also shown. Finally, position of each cell along the SCP-to-chromaffin differentiation trajectory pseudotime is shown in the last plot. **D.** Expression profiles of 1480 genes (rows) that are statistically significantly associated with the differentiation trajectory are shown as a function of pseudotime (cell position, x axis; individual cells colored according to their cluster membership are shown right below the axis). The genes can be categorized into those expressed early (close to SCPs), late (close to chromaffin) and transiently (within the"bridge"subpopulation). **E.** Examples of pseudotime expression profiles for key genes within each category. Each point represents a cell, with the small horizontal line around it indicating uncertainty (95% CI) of the cell's position within the differentiation pseudotime. A smoothed regression line with the associated 95% CI is shown in red. **F-J.** Analogous subpopulation and SCP-to-chromaffin differentiation"bridge"can be seen in the neural crest-derived cells of the E13.5 adrenal medulla. In panel A, the greyscale gradient represents z-scores from 4.3 to 63, while in panel F from 5 to 105. K, L. t-SNE plots of developing medulla subpopulations normalized for the cell cycle-correlated genes at E12.5 (**K**) and E13.5 (**L**). Note that yellow population aligns with the red "bridge" population. The graphs show the fraction of cells undergoing mitosis (y-axis) as a function of pseudotime. Cells were classified as mitotic in the case of a positive score on the mitosis-driven aspect of heterogeneity.
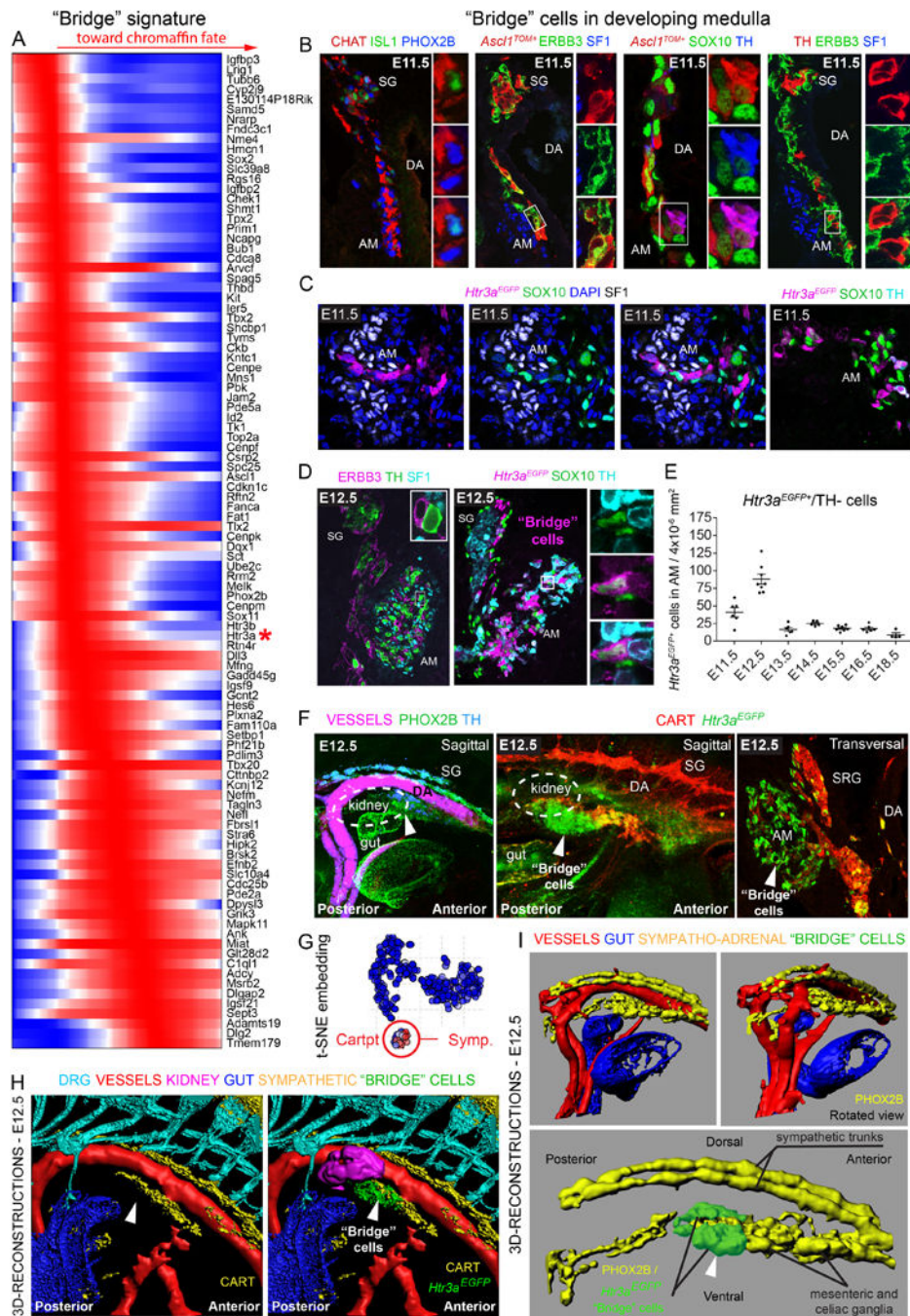
Fig. 6. Mapping a novel "bridge" population of cells to the anatomical location and developmental timeline

A. Genes in the "bridge" cell population whose expression is dynamically changing in a statistically significant way. **B.** Left: immunohistochemistry for CHAT, PHOX2B and ISL1 on sections of adrenal medulla (AM) region from E11.5 embryos. Note that PHOX2B^{+} cells are associated with CHAT[+] nerve. Center: in 24h-traced $Ascl1^{CreERT2/+};R26R^{TOM/TOM}$ embryos analyzed at E11.5, nerve-associated cells of the intermediate stage express $Ascl1$ in addition to the glial markers ERBB3 and SOX10. Note that TH[+]/$Ascl1^{TOM+}$ cells retain low

levels of SOX10. Right: immunohistochemistry at E11.5 for TH, ERBB3 and SF1 shows that TH$^+$ cells near the assembling adrenal cortex (SF1$^+$ cells) are associated with the nerve but do not express glial markers. **C-D.** Validation of the "bridge" cell population in SCP-to-chromaffin transition marked by the expression of *Htr3a*^{EGFP} in E11.5 (**C**) and E12.5 (**D**) embryos. In **C**, immunohistochemistry for GFP (recapitulating *Htr3a* expression), SOX10 and SF1 shows the anatomical position of the very first *Htr3a*^{EGFP} AM cells within the developing adrenal gland region (marked by SF1 expression). Right: immunohistochemistry for GFP (recapitulating *Htr3a* expression), SOX10 and TH shows that intermediate "bridge" *Htr3a*^{EGFP} cells of AM rarely express TH but retained variable levels of SOX10. In **D**, AM cells are either intermediate "bridge" TH$^+$/*Htr3a*^{EGFPlow} and SOX10$^+$/*Htr3a*^{EGFPlow} or chromaffin TH$^+$/*Htr3a*$^{EGFP-}$ cells. **E.** *Htr3a*$^{EGFP+}$ cells number in the medulla region peaks at E12.5, declines at E13.5 and keeps constant throughout development. Each dot represents counts from one medullary region (n=2 embryos for all ages). **F.** Left panel: whole mount immunofluorescence for PHOX2B and TH (magenta: auto-fluorescent blood vessels), CART and *Htr3a*^{EGFP} (middle panel) and immunohistochemistry on transversal cryosection (right panel). **G.** Note that *Cartpt* (gene coding for CART) is not expressed in the intermediate *Htr3a*$^{EGFP+}$ "bridge" cells or differentiating chromaffin cells, while it is present in sympathetic neurons of the SRG. **H, I.** Corresponding 3D-reconstructions of sympatho-adrenal structures of E12.5 embryos. Large blood vessels were reconstructed based on blood vessel auto-fluorescence of embryonic erythrocytes (see F). Sympathetic structures were reconstructed based on CART$^+$ and PHOX2B$^+$ signal. Note the consolidation of ventral sympathetic structures (presumably SRG, para-aortic, future mesenteric and celiac ganglia) at this stage as well as the presence of the intermediate "bridge" cells outlined in the AM by *Htr3a*^{EGFP} signal (white arrows). SG: sympathetic ganglion; DA: dorsal aorta; AM: adrenal medulla; SRG: suprarenal ganglion.